SIAM J. APPL. MATH.
Vol. 71, No. 4, pp. 1428–1457

STABILITY OF SPIKY SOLUTIONS IN A COMPETITION MODEL WITH CROSS-DIFFUSION*

THEODORE KOLOKOLNIKOV† AND JUNCHENG WEI‡

Abstract. We consider the Shigesada–Kawasaki–Teramoto model of species segregation in the limit of high cross-diffusion rate of one species, and small diffusion rate of another. Recently, steady states in the shape of an inverted spike were constructed in this limit in one dimension [Y. Lou, W.-M. Ni, and S. Yotsutani, *Discrete Contin. Dyn. Syst.*, 10 (2004), pp. 435–458; Y. Wu and Q. Xu, *Discrete Contin. Dyn. Syst.*, 29 (2011), pp. 367–385]. In this paper we consider the stability properties of such spiky states. We show that K symmetric spikes are stable if the domain length is sufficiently large. More precisely, we derive a sequence of thresholds $0 = L_1 < L_2 < L_3 < L_4 < L_5 \dots$ such that K spikes on the domain of size $2KL$ are stable if and only if $L > L_K$. When $K = 2$, the instability of a small eigenvalue is triggered first, resulting in a very slow drift of the two spikes, with eventual absorption of one by the other. When $K \geq 3$, the primary instability is due to a large eigenvalue, resulting in a quick death of one or more spikes. We also extend the construction of one-dimensional steady states to a radially symmetric two-dimensional spike at the center of a disk. In one dimension, hypergeometric functions are utilized to study the large eigenvalues; thresholds for small eigenvalues are derived indirectly by classifying the bifurcations of asymmetric patterns. Full numerical simulations in one and two dimensions are performed to confirm the asymptotic results and to explore some of the dynamical scenarios away from the equilibrium state.

Key words. partial differential equations, reaction diffusion, cross diffusion, spikes, pattern formation, stability

AMS subject classifications. 35K57, 35B36, 35B40

DOI. 10.1137/100808381

1. Introduction.

Back in 1979, Shigesada, Kawasaki, and Teramoto proposed the following reaction-diffusion system to model segregation phenomena in population dynamics [20]:

$$\begin{cases} u_t = \Delta\left[(d_1 + \rho_{12} v)\, u\right] + u(a_1 - b_1 u - c_1 v), \\ v_t = \Delta\left[(d_2 + \rho_{21} u)\, v\right] + v(a_2 - b_1 u - c_1 v). \end{cases} \tag{1.1}$$

Here, u, v represent the densities of the two competing species, and all parameters are assumed positive. Without the spatial diffusion terms, this is just the classical Lotka–Volterra ODE system. The terms d_1 and d_2 model the usual self-diffusion, while the cross-diffusion terms ρ_{12} and ρ_{21} model the interspecies avoidance: upon spatial encounter, the species tend to disperse away from each other.

The interspecies avoidance has been documented, for example, among cheetahs, lions, and hyenas [2], [3]. Durant in [2] demonstrated that *"lion avoidance [among cheetah] translated into a nonrandom spatial distribution of cheetahs with the most reproductively successful females found near lower lion densities than less successful females."* In [3], cheetah were shown to actively move away upon hearing the recordings of lions. Durant in [3] proposed that this mechanism helps to sustain the cheetah

*Received by the editors September 13, 2010; accepted for publication (in revised form) April 27, 2011; published electronically August 11, 2011.
http://www.siam.org/journals/siap/71-4/80838.html
†Mathematics and Statistics, Dalhousie University, Halifax, NS B3H 3J5, Canada (tkolokol@mathstat.dal.ca). This author is supported by NSERC discovery grant 47050, Canada.
‡Department of Mathematics, Chinese University of Hong Kong, Shatin, Hong Kong (wei@math.cuhk.edu.hk). This author is partially supported by GRF of RGC Hong Kong, and by Joint Overseas Grant of NSFC.

populations, since (a) cheetah cubs are actively preyed upon by lions, and (b) cheetah and lions compete for the same prey.

Since the introduction of (1.1), various regimes have been studied in numerous papers; see, for example, [15], [16], [17], [12], [13], [11], [26], [25]. Of particular importance is understanding the effect of the cross-diffusion rates ρ_{12}, ρ_{21}. In fact, as was shown in [8], any nonconstant solution is unstable in the absence of cross-diffusion ($\rho_{12} = 0 = \rho_{21}$). This is true in any dimension, at least for rectangular domains (including a one dimensional interval), and is conjectured in [8] to be true for any convex domain.

In this paper we consider a simplified version of (1.1), where one of the cross-diffusion coefficients is much bigger than the other. This simplification was first introduced in [16]; without loss of generality, we may assume that ρ_{12} is dominant. Following [11] and [26] we also discard d_1 and ρ_{21} and consider as a starting point the following system:

$$\text{(1.2)} \qquad \begin{cases} u_t = \rho\,(vu)_{xx} + a_1 u - b_1 u^2 - c_1 uv \\ v_t = dv_{xx} + a_2 v - b_2 uv - c_2 v^2 \end{cases} ; \qquad a \le x \le b,$$
$$u_x(a,t) = 0 = u_x(b,t), \quad v_x(a,t) = 0 = v_x(b,t),$$

where

$$d := d_2, \quad \rho := \rho_{12}, \quad d_1 = \rho_{21} = 0,$$

and as in [26], we furthermore assume the following asymptotic regime:

$$\text{(1.3)} \qquad d \ll 1, \quad \rho \gg 1, \quad \text{all other parameters are positive and of } O(1).$$

Biologically, when ρ is large, v acts as an inhibitor on u so that u diffuses quickly in the regions of high concentration of v. This effect is believed to be responsible for the segregation of the two species. It was shown in [11] and [26] that under these assumptions, the system (1.2) may admit a steady state *in the form of a spike* for u, and in the form of an inverted spike for v. An example of such a solution is shown in Figure 1. Note in particular that within the spike for u, the population of v is very low. This spatial pattern is the result of the interspecies avoidance.

The main goal of this paper is to study the stability properties of the spiky solutions of (1.2) that were constructed in [11], [26]. A secondary goal is to extend the computations of the steady state in [26] to two dimensions. Let us first mention some of the previous results concerning the nonconstant steady states of (1.1) and their stability. In [16], Mimura et al. constructed nonconstant steady states *consisting of interfaces* (also called mesa patterns) for (1.1) under the assumption that $\rho_{21} = 0$. Numerically, some have been observed to be stable. The stability was further analyzed in [7] using the SLEP (singular limit eigenvalue problem) method. With regard to *spike-type solutions*, several of these were constructed in [11], [12], [13] in one dimension and under various assumptions on parameters; we are not aware of any results concerning spikes for (1.1) in two dimensions. In [25], some of the spike solutions were proven to be *unstable*; no stable spikes were found. In light of the instability result in [25] it is natural to ask, *Does there exist a regime for which spike-type solutions are stable?* In this paper, we not only answer this in the affirmative but also give a full characterization of the instability thresholds. In addition, we construct the spiky steady states in two dimensions. To our knowledge, this is the first demonstration of stable spikes for this model; the construction of solutions in two dimensions is also new.

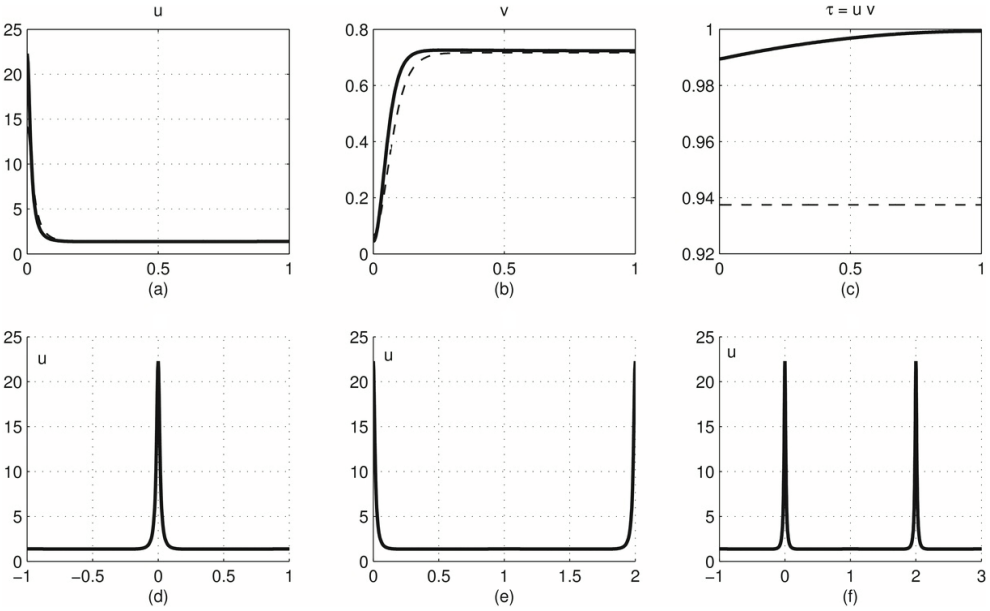

FIG. 1. *Steady states configurations considered in this paper.* (a), (b), (c): *Half-spike on* $[0, L]$. *Both* u *and* v *have boundary layers at zero, whereas* $\tau = uv$ *is nearly constant. Note that* $v(0)$ *is small and* $u(0)$ *is large. Solid line shows the full numerical computation; asymptotic approximations derived in Proposition* 2.1 *are shown using dashed lines. Parameter values are* $d_2 = 4 \times 10^{-3}$, $\rho = 200$, $(a_1, b_1, c_1) = (5, 1, 1)$, $(a_2, b_2, c_2) = (5, 1, 5)$, *and* $L = 1$. (d) *A single interior spike.* (e) *A double-boundary spike configuration.* (f) *a two-spike configuration (i.e.,* $L = 1$, $K = 2$*).*

We now summarize the main stability result of this paper. We consider stability of the following spiky states (see Figure 1):

(i) A boundary spike at 0 on the interval $[0, L]$;

(ii) a double boundary spike configuration, consisting of two boundary spikes at 0 and at $2L$ on a domain $[0, 2L]$;

(iii) K interior spikes on the domain $[-L, (2K-1)L]$, whose centers are located at $0, 2L, 4L, \ldots, 2(K-1)L$.

Note that the steady states (ii) and (iii) are trivially constructed from (i) by appropriate reflections and translations. The basic spike (i) has a property that $v(0)$ is very close to zero, whereas $u(0)$ is large. Such a large spike solution was first shown to exist in [11]; more detailed asymptotics, including its height, were computed in [26]. We review their construction in section 2 (see Proposition 2.1).

While (ii), (iii) are trivially constructed from (i), the stability properties of (i), (ii), and (iii) are very different. This is illustrated in Figure 2. Our main result is the precise characterization of their stability. We summarize it as follows.

PRINCIPAL RESULT 1.1. *Suppose that*

$$4\frac{a_1}{a_2} - \frac{b_1}{b_2} - 3\frac{c_1}{c_2} > 0, \tag{1.4}$$

and consider a spike steady state as constructed in Proposition 2.1. *Define*

$$\varepsilon := \sqrt{2d/a_2},$$

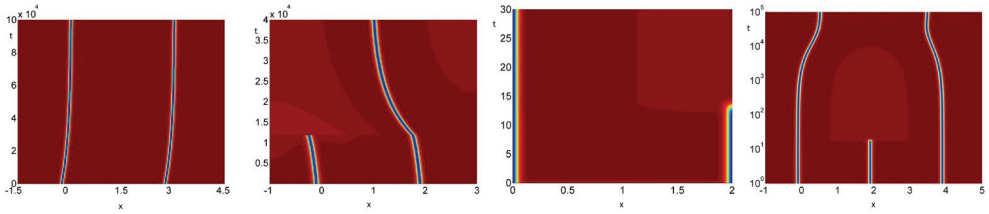

(a) (b) (c) (d)

FIG. 2. *Various instabilities of Principal Result* 1.1. (a) *Two stable spikes. Parameter values in* (1.2) *are* $d_2 = 10^{-3}$; $\rho = 200$; $(a_1, b_1, c_1) = (5, 1, 1)$; $(a_2, b_2, c_2) = (5, 1, 5)$; *and* $L = 1.5$, $K = 2$ *with* $b - a = 2KL$. (b) *Slow instability. Two spikes persist as a transient state until* $t \sim 1.2 \times 10^4$. *Parameter values are the same as in* (a) *except that* $L = 1$. (c) *Fast instability of two boundary spikes. Parameter values are the same as in* (b), *except that* $b - a = 2$. (d) *Fast instability of three spikes (note log time scale). The middle spike disappears at* $t \sim 20$. *The remaining two spikes slowly drift towards a symmetric equilibrium. Parameter values are the same as in* (b) *except* $K = 3$.

$$\rho_{K,small} := \varepsilon^{-2/3} L^{8/3} \frac{c_2}{2} \left(\frac{b_1}{b_2} \frac{\pi}{2} \right)^{-2/3} \left(4\frac{a_1}{a_2} - \frac{b_1}{b_2} - 3\frac{c_1}{c_2} \right)^{5/3}, \tag{1.5}$$

$$\rho_b := \frac{1}{2\chi_c} \rho_{K,small}, \quad \text{where } \chi_c = 0.669 \text{ is as determined in Principal Result 4.2,} \tag{1.6}$$

$$\rho_{K,large} := \rho_{K,small} \frac{1}{(1 - \cos[\pi(1 - 1/K)])\chi_c}. \tag{1.7}$$

We have the following conclusions:

- *A single boundary spike* (i) *is stable for all* ρ.
- *A double-boundary steady state* (ii) *is stable if* $\rho < \rho_b$ *and is unstable otherwise. The instability is due to a large eigenvalue.*
- *A* K *interior spike steady state* (iii) *with* $K \geq 2$ *is stable if* $\rho < \min(\rho_{K,small}, \rho_{K,large})$ *and is unstable otherwise. When* $K = 1$, *it is stable provided that* ρ *is not exponentially large in* ε.

Several remarks are in order. First, there are two distinct types of instabilities that can occur: either small or large eigenvalues can be destabilized. The instability with respect to small eigenvalues typically results in a slow drift of one or more spikes, and eventually may lead to spike death over a long time. This is illustrated, for example, in Figure 2(b). On the other hand, the instability with respect to a large eigenvalue, also called competition instability, results in spike death that occurs at $O(1)$ time. This is illustrated in Figure 2(c),(d).

Our second remark is that the critical scaling for the instability thresholds for both small and large eigenvalues is

$$\rho = O(d^{-1/3}). \tag{1.8}$$

In particular, K spikes are always stable whenever $1 \ll \rho \ll d^{-1/3}$ (since in this case $\rho < \rho_{K,\text{small}}$ and $\rho < \rho_{K,\text{large}}$) and are unstable when $K \geq 2$ and $\rho \gg d^{-1/3}$ (since in this case $\rho > \rho_{K,\text{small}}$ and $\rho > \rho_{K,\text{large}}$, so both small and large eigenvalues become unstable). Finally, note that

$$\frac{1}{(1 - \cos[\pi(1 - 1/K)])\chi_c} = \begin{cases} 1.494, & K = 2, \\ 0.996, & K = 3, \\ 0.875, & K = 4, \end{cases}$$

so that $\rho_{K,\text{large}} > \rho_{K,\text{small}}$ if $K = 2$ but $\rho_{K,\text{large}} < \rho_{K,\text{small}}$ if $K \geq 3$. It follows that the primary instability is due to small eigenvalues if $K = 2$ but is due to large eigenvalues if $K \geq 3$. This is in agreement with numerical simulations, some of which are shown in Figure 2 (see also section 7, Experiment 3).

The outline of this paper is as follows. In section 2 we review the construction of the steady state (Proposition 2.1). A similar computation was performed in [26] where, in particular, the height $u(0)$ was also derived; however, we simplify it significantly here in that we avoid using certain complicated exact integrals as was done in [26] (this simplification also allows us to construct the solution in two dimensions in section 6, where such exact integrals are no longer available). The main stability result is then derived in sections 3–5. For the spiky patterns, there are two types of eigenvalues that need to be considered: so-called large and small eigenvalues. In section 3 we first derive the reduced eigenvalue problem for the large eigenvalues. We then use hypergeometric functions to study it in section 4. In section 5 we turn our attention to the instability due to small eigenvalues. Rather than computing the small eigenvalues directly, we derive only their instability thresholds. This is done by calculating the bifurcation point at which asymmetric spike patterns bifurcate off the solution branch corresponding to spikes of equal height. In analogy to studies of similar models such as the Gierer–Meinhardt (GM) system [4], [19], we expect the small eigenvalues to become unstable at these bifurcation points. This is verified numerically. Radially symmetric steady states inside a two-dimensional disk are constructed in section 6. In section 7 we perform full numerical simulations in one and two dimensions to confirm our asymptotic results. Finally, in section 8 we discuss our results and present some future directions.

The methods used in this paper are based on formal asymptotics. The critical computation in section 4 showing that stability of the large eigenvalues involves the hypergeometric functions had to be done numerically. It remains an open challenge to provide a rigorous foundation, especially for the key step in section 4.

2. Steady state computation in one dimension. Before stating our stability results, let us summarize the asymptotic shape of the spiky steady state, which was first considered in [11], [26].

PROPOSITION 2.1 (see [26]). *Consider the steady state equations*

$$0 = dv_{xx} + a_2 v - b_2 uv - c_2 v^2, \qquad 0 = \rho\,(vu)_{xx} + a_1 u - b_1 u^2 - c_1 uv \tag{2.1}$$

on the interval $[0, L]$ *with Neumann boundary conditions. Suppose that*

$$4\frac{a_1}{a_2} - \frac{b_1}{b_2} - 3\frac{c_1}{c_2} > 0, \tag{2.2}$$

and consider the asymptotic limit

$$d \ll 1, \quad \rho \gg 1. \tag{2.3}$$

The system (2.1) *admits a solution such that* $v(x)$ *has the form of an inverted spike at* $x = 0$*, with its minimum close to zero. More precisely, we have*

$$v(x) \sim \frac{a_2}{2c_2}\left[\frac{3}{2}\tanh^2\left(\frac{x}{2\varepsilon}\right) + \delta\left(2 - 3\tanh^2\left(\frac{x}{2\varepsilon}\right)\right)\right], \tag{2.4}$$

$$u \sim \frac{\tau_0}{v(x)}, \tag{2.5}$$

where

$$\varepsilon := \sqrt{\frac{2d}{a_2}}, \tag{2.6}$$

$$\tau_0 := \frac{3}{16}\frac{a_2^2}{b_2 c_2}, \tag{2.7}$$

$$\delta := \left(\frac{\varepsilon}{L}\right)^{2/3} \frac{3}{4}\left(\frac{b_1}{b_2}\frac{\pi}{2}\right)^{2/3}\left(4\frac{a_1}{a_2} - \frac{b_1}{b_2} - 3\frac{c_1}{c_2}\right)^{-2/3}. \tag{2.8}$$

Note that the solution given by (2.4), (2.5) is valid uniformly throughout the entire interval $[0, L]$. An example of this is shown in Figure 1.

We define

$$\tau = uv,$$

and replacing $u = \tau/v$ in (2.1) we obtain

$$0 = dv_{xx} + a_2 v - b_2\tau - c_2 v^2, \tag{2.9}$$

$$0 = \rho\tau_{xx} + \tau\left(\frac{a_1}{v} - b_1\frac{\tau}{v^2} - c_1\right), \tag{2.10}$$

with Neumann boundary conditions for v and τ on $[0, L]$. Due to the assumption $\rho \gg 1$, to leading order, we have $\tau_{xx} = 0$ so that Neumann boundary conditions imply that $\tau(x) \sim \tau_0$ is constant throughout the domain, with τ_0 to be determined. Upon integrating (2.10) on $[0, L]$, we then obtain an integral constraint

$$\int_0^L \tau\left(\frac{a_1}{v} - b_1\frac{\tau}{v^2} - c_1\right) dx = 0. \tag{2.11}$$

Estimating $\tau(x) \sim \tau_0$, we then obtain the leading order constraint

$$Lc_1 \sim \int_0^L \left(\frac{a_1}{v} - b_1\frac{\tau_0}{v^2}\right) dx. \tag{2.12}$$

To satisfy this constraint, we seek solutions for $v(x)$ in the form of an inverted spike such as shown in Figure 1, so that $v(0)$ is very close to zero. In order to construct such a solution, consider the unique ground state solution

$$w(y) = \frac{3}{2}\operatorname{sech}^2\left(\frac{y}{2}\right) \tag{2.13}$$

to the problem

$$w_{yy} - w + w^2 = 0, \quad w \to 0 \text{ as } |y| \to \infty, \quad w'(0) = 0, \quad w > 0. \tag{2.14}$$

Next, define

$$V_0(y) := \frac{3}{2} - w(y) = \frac{3}{2}\tanh^2\left(\frac{y}{2}\right)$$

so that $V_0(y)$ satisfies

$$V_{0yy} + 2V_0 - V_0^2 - \frac{3}{4} = 0; \quad V_0(0) = 0,\ V_0'(0) = 0, \quad V_0 \to \frac{3}{2} \text{ as } |y| \to \infty. \tag{2.15}$$

We now scale v and x so that the leading order of (2.9) can be mapped into (2.15). In the inner region we let

$$v = \alpha V(y), \quad x = \varepsilon y,$$

where ε is the extent of the inner layer to be determined. Then (2.9) becomes

$$0 = d\varepsilon^{-2} V_{yy} + a_2 V - b_2 \tau/\alpha - c_2 \alpha V^2.$$

In the inner region, we expand the solution as

$$V = V_0 + \varepsilon^p V_1 + \cdots, \quad \tau = \tau_0 + \varepsilon^p \tau_1 + \cdots, \tag{2.16}$$

where the power $p > 0$ is to be determined. The leading order equation for V_0 in the inner region is

$$d\varepsilon^{-2} V_{0yy} + a_2 V_0 - b_2 \tau_0/\alpha - c_2 \alpha V_0^2 = 0.$$

Matching to (2.15) we have

$$\frac{a_2 \varepsilon^2}{d} = 2, \quad \frac{b_2 \tau_0 \varepsilon^2}{\alpha d} = \frac{3}{4}, \quad \frac{c_2 \alpha \varepsilon^2}{d} = 1,$$

so that

$$\varepsilon = \sqrt{\frac{2d}{a_2}}, \quad \tau_0 = \frac{3}{16} \frac{a_2^2}{b_2 c_2}, \quad \alpha = \frac{a_2}{2c_2}.$$

Thus, at leading order, we obtain

$$v(x) \sim \frac{a_2}{2c_2} V_0\left(\frac{x}{\varepsilon}\right), \quad \varepsilon = \sqrt{\frac{2d}{a_2}}, \quad V_0(y) = \frac{3}{2} \tanh^2\left(\frac{y}{2}\right).$$

Going back to the full problem, note that $u(x) \sim \tau_0/v(x)$ also has a form of the spike; however, to determine its height $u(0)$, it is necessary to find the corrections to $v(0)$. Therefore it is necessary to compute V_1. We have

$$V_{1yy} + 2V_1 - 2V_0 V_1 - 4\frac{b_2 c_2}{a_2^2} \tau_1 = 0, \qquad \tau_{1yy} = 0, \tag{2.17}$$

so that τ_1 is constant. We write (2.17) as

$$L_0 V_1 = \delta_0, \tag{2.18}$$

where

$$\delta_0 \equiv 4\frac{b_2 c_2}{a_2^2} \tau_1 \tag{2.19}$$

and

$$L_0 \Phi \equiv \Phi_{yy} - \Phi + 2\Phi w$$

is the operator that arises from the linearization of the ground state (2.14). To solve (2.18), note the following identities:

$$L_0(1) = -1 + 2w, \qquad L_0\left(\frac{y w_y}{2} + w\right) = w \tag{2.20}$$

so that

$$V_1 = -\delta_0 + 2\delta_0 \left(\frac{y w_y}{2} + w \right).$$

Thus, to two orders, we obtain,

(2.21)
$$V \sim \frac{3}{2} \left(\tanh^2 \left(\frac{y}{2} \right) \right) + \delta \left(2 - 3 \tanh^2 \left(\frac{y}{2} \right) - \frac{3}{2} y \tanh \left(\frac{y}{2} \right) \operatorname{sech}^2 \left(\frac{y}{2} \right) \right) + O\left(\delta^2\right),$$

where

$$\delta \equiv \delta_0 \varepsilon^p = 4 \frac{b_2 c_2}{a_2^2} \tau_1 \varepsilon^p. \tag{2.22}$$

Note that (2.21) is valid uniformly throughout the domain $y \in [0, L/\varepsilon]$. It remains to determine $\varepsilon^p \tau_1$. To do so, we use the solvability condition (2.12). We start by evaluating

$$\int_0^L \frac{a_1}{v} dx = \frac{2 c_2 a_1}{a_2} \int_0^L \frac{1}{V} dx.$$

We choose a number σ with $\varepsilon \delta^{1/2} \ll \sigma \ll \varepsilon$ and split the integration range as

$$\int_0^L \frac{1}{V} dx \sim \int_0^\sigma \frac{1}{V} dx + \int_\sigma^L \frac{1}{V} dx.$$

To evaluate $\int_0^\sigma \frac{1}{V(x)} dx$, we make a change of variables $x = \delta^{1/2} \varepsilon z$. By assumption $\sigma \ll \varepsilon$, we have $y \ll 1$, so we expand (2.21) in Taylor series to obtain

$$V \sim \delta \left(\frac{3}{8} z^2 + 2 \right) + O(\delta^2). \tag{2.23}$$

We then obtain

$$\int_0^\sigma \frac{1}{V} dx \sim \delta^{1/2} \varepsilon \int_0^{\frac{\sigma}{\varepsilon \delta^{1/2}}} \frac{dz}{\delta \left(\frac{3}{8} z^2 + 2 \right)} \sim \varepsilon \delta^{-1/2} \frac{8}{3} \left(\int_0^\infty \frac{dz}{z^2 + \frac{16}{3}} - \int_{\frac{\sigma}{\varepsilon \delta^{1/2}}}^\infty z^{-2} \right)$$

$$\sim \frac{\pi}{\sqrt{3}} \frac{\varepsilon}{\sqrt{\delta}} - \frac{\varepsilon^2}{\sigma} \frac{8}{3}. \tag{2.24}$$

On the other hand, to estimate $\int_\sigma^L \frac{1}{V} dx$, note that by assumption $\sigma \gg \varepsilon \delta^{1/2}$, we have $y \gg \delta^{1/2}$ and $\tanh^2(y/2) \gg \delta$, so that $V \sim \frac{3}{2} \tanh^2 (y/2)$. We then estimate

$$\int_\sigma^L \frac{1}{V} dx \sim \frac{2}{3} \varepsilon \int_{\sigma/\varepsilon}^{L/\varepsilon} \frac{1}{\tanh^2 (y/2)} dy.$$

The integral on the right-hand side has the following asymptotics:

$$\int_m^M \frac{dy}{\tanh^2 (y/2)} \sim M + \frac{4}{m} + O(1) \quad \text{in the limit } M \gg 1 \text{ and } m \ll 1. \tag{2.25}$$

To show (2.25), we add and substract $(y/2)^{-2}$ from the integrand to split off the singularity. Let a be any number with $1 \ll a \ll M$. We have,

$$\begin{aligned}\int_m^M \frac{dy}{\tanh^2(y/2)} &= \int_m^M \left(\frac{1}{\tanh^2(y/2)} - \frac{4}{y^2}\right) dy + \int_m^M \frac{4}{y^2} dy \\ &\sim \int_m^a \left(\frac{1}{\tanh^2(y/2)} - \frac{4}{y^2}\right) dy + \int_a^M dy + \frac{4}{m} + O(M^{-1}) \\ &\sim O(a) + M + \frac{4}{m}.\end{aligned}$$

Taking the limit $a \to O(1)$ we obtain (2.25). (Alternatively, an exact formula for the indefinite integral $\int ds/\tanh^2(s)$ is available, from which (2.25) can be explicitly derived.) Thus we obtain

$$\int_\sigma^L \frac{1}{V} dx \sim \frac{2}{3}\varepsilon\left(\frac{L}{\varepsilon} + \frac{4\varepsilon}{\sigma}\right). \tag{2.26}$$

Adding (2.24) and (2.26) together, note that *the terms involving σ in* (2.24) *and* (2.26) *cancel each other out* so that we obtain the asymptotic result

$$\int_0^L \frac{1}{V} dx \sim \frac{\pi}{\sqrt{3}}\frac{\varepsilon}{\sqrt{\delta}} + \frac{2}{3}L,$$

which is independent σ (as it should be). In a similar manner, we compute

$$\int_0^L b_1 \frac{\tau_0}{v^2} dx = \frac{3}{4}\frac{b_1}{b_2} c_2 \int_0^L \frac{1}{V^2} dx$$

and

$$\begin{aligned}\int_0^L \frac{1}{V^2} dx &\sim \varepsilon\delta^{-3/2} \int_0^\infty \frac{dz}{\left(\frac{3}{8}z^2 + 2\right)^2} + \frac{4}{9}L \\ &\sim \frac{1}{12}\sqrt{3}\delta^{-3/2}\varepsilon\pi + \frac{4}{9}L,\end{aligned}$$

where we have used the fact that $\int_0^\infty \frac{dy}{(y^2+a)^2} = a^{-3/2}\frac{\pi}{4}$. Thus to leading order, we get

$$\begin{aligned}Lc_1 &\sim \frac{c_2 a_1}{a_2}\left(\frac{2\pi}{\sqrt{3}}\frac{\varepsilon}{\sqrt{\delta}} + \frac{4}{3}L\right) - \frac{3}{4}\frac{b_1}{b_2}c_2\left(\frac{1}{12}\sqrt{3}\delta^{-3/2}\varepsilon\pi + \frac{4}{9}L\right), \\ \frac{b_1}{b_2}\frac{1}{16}\sqrt{3}\delta^{-3/2}\varepsilon\pi &\sim \frac{1}{3}\left(4\frac{a_1}{a_2} - \frac{b_1}{b_2} - 3\frac{c_1}{c_2}\right)L, \\ \delta &\sim \frac{3}{4}\left(\frac{b_1}{b_2}\frac{\pi}{2}\right)^{2/3}\left(4\frac{a_1}{a_2} - \frac{b_1}{b_2} - 3\frac{c_1}{c_2}\right)^{-2/3}\left(\frac{\varepsilon}{L}\right)^{2/3}.\end{aligned}$$

Recalling (2.22) we then obtain

$$p = \frac{2}{3} \tag{2.27}$$

and

$$\tau_1 = \frac{3}{16}\frac{a_2^2}{b_2 c_2}\left(\frac{b_1}{b_2}\frac{\pi}{2}\right)^{2/3}\left(4\frac{a_1}{a_2} - \frac{b_1}{b_2} - 3\frac{c_1}{c_2}\right)^{-2/3} L^{-2/3}. \tag{2.28}$$

This completes the construction of the steady state. ∎

3. Stability; large eigenvalues. Next we consider the stability. After change of variables $\tau = uv$, the full equations (1.2) become

$$v_t = dv_{xx} + a_2 v - b_2 \tau - c_2 v^2,$$
$$\left(\frac{\tau}{v}\right)_t = \rho \tau_{xx} + \tau\left(\frac{a_1}{v} - b_1 \frac{\tau}{v^2} - c_1\right).$$

We linearize around the steady state $v(x), \tau(x)$:

$$v(x,t) = v(x) + e^{\lambda t}\phi(x), \quad \tau(x,t) = \tau(x) + e^{\lambda t}\psi(x).$$

The linearized equations are

$$\lambda\phi = d\phi_{xx} + a_2\phi - b_2\psi - c_2 2v\phi, \tag{3.1}$$

$$\lambda\left(\frac{1}{v}\psi - \frac{\tau}{v^2}\phi\right) = \rho\psi_{xx} + \left(\frac{a_1}{v} - b_1 2\frac{\tau}{v^2} - c_1\right)\psi + \left(-\frac{a_1\tau}{v^2} + 2b_1\frac{\tau^2}{v^3}\right)\phi. \tag{3.2}$$

The stability analysis consists of looking at both small and large eigenvalues. In this section, we construct the reduced eigenvalue problem for the large eigenvalues, which are the eigenvalues with $\lambda \to \lambda_0 \neq 0$ as $\varepsilon \to 0$. The reduced problem is independent of the small diffusion d, and it is then analyzed in more detail in section 4. On the other hand, the small eigenvalues arise due to translation invariance of the inner problem and satisfy $\lambda \to 0$ as $d \to 0$. The stability with respect to small eigenvalues is studied indirectly in section 5 by determining the parameter values for which the asymmetric spike patterns bifurcate off the symmetric branch, and without actually computing the small eigenvalues themselves.

Two boundary spikes. We first consider a steady state that consists of two boundary spikes on the domain $[0, 2L]$ (that is, a half-spike on $[0, L]$ reflected in the line $x = L$, as shown in Figure 1(e)). Such a configuration admits two distinct eigenfunctions: one is even about $x = L$ and another is odd about $x = L$. The former corresponds to the boundary conditions $\phi'(L) = \psi'(L) = 0$, whereas the latter corresponds to the boundary conditions $\phi(L) = \psi(L) = 0$; both have Neumann boundary conditions at the origin: $\phi'(0) = \psi'(0) = 0$.

In the outer region $\varepsilon \ll x < L$ away from the spike at $x = 0$, we drop the term $d\phi_{xx}$. We then obtain

$$\phi \sim \left(\frac{b_2}{a_2 - 2c_2 v^\star - \lambda}\right)\psi, \qquad \psi_{xx} \sim 0,$$

where $v^\star \equiv \frac{3a_2}{4c_2}$ is the leading order behavior of $v(x)$ in the outer limit, obtained by taking $x \gg O(\varepsilon)$ in (2.4). We then obtain

$$\phi \sim \frac{-b_2}{a_2/2 + \lambda}\psi.$$

In the inner region, we change variables as in section 2,

$$v(x) \sim \frac{a_2}{2c_2}V(y), \quad y = \frac{x}{\varepsilon},$$
$$\phi(x) = \Phi(y), \quad \psi(x) = \Psi(y).$$

We then obtain, to leading order, that $\Psi_{yy} = 0 \implies \Psi(y) = \Psi_0$ is a constant and that

$$\lambda\frac{2}{a_2}\Phi = \Phi_{yy} + (-1 + 2w)\,\Phi - \frac{2b_2}{a_2}\Psi_0.$$

We now determine Ψ_0 by matching the inner and outer regions.

First, consider the eigenfunction which is odd at L, that is, $\psi(L) = 0$. The matching condition is that $\psi(x) \to \Psi_0$ as $x \to 0$. Solving in the outer region for $\rho \gg 0$, we have $\psi_{xx} \sim 0$ so that

$$\psi \sim \frac{1}{L}(L-x)\Psi_0. \tag{3.3}$$

As before, choose a number σ with $\varepsilon\delta^{1/2} \ll \sigma \ll \varepsilon$, and integrate (3.2) on the interval $[0,\sigma]$. Using $\psi'(0) = 0$, we then obtain, to leading order,

$$\rho\psi'(\sigma) + 2b_1\tau^2 \int_0^\sigma \frac{\phi}{v^3} \sim 0, \tag{3.4}$$

while matching with (3.3) we also get

$$\psi'(\sigma) = -\Psi_0/L. \tag{3.5}$$

Next we estimate the integral as follows:

$$\begin{aligned} I = \int_0^\sigma \frac{\phi}{v^3} &\sim \left(\frac{2c_2}{a_2}\right)^3 \varepsilon \int_0^\infty \frac{\Phi(y)dy}{(V(y))^3} \\ &\sim \left(\frac{2c_2}{a_2}\right)^3 \varepsilon \int_0^\infty \frac{\Phi(y)dy}{\left(\frac{3}{8}y^2 + 2\delta\right)^3}, \end{aligned}$$

where $\delta \ll 1$ is defined as in (2.8). We change the variables $y = \sqrt{\delta}z$, $\delta \ll 1$, and obtain

$$\begin{aligned} I &\sim \left(\frac{2c_2}{a_2}\right)^3 \Phi(0)\delta^{-5/2}\varepsilon \int_0^\infty \frac{dz}{\left(\frac{3}{8}z^2 + 2\right)^3} \\ &\sim \frac{c_2^3}{a_2^3}\delta^{-5/2}\varepsilon\pi\frac{\sqrt{3}}{4}\Phi(0). \end{aligned}$$

(Above, we estimated $\Phi(z) \sim \Phi(0)$, since in the z variable, the leading order equation for Φ becomes $\Phi_{zz} \sim 0$, so that Φ is constant for the extent of z.) Combining (3.4), (3.5), and (2.7) we obtain

$$\begin{aligned} \Psi_0 &= -L\psi'(\sigma) \\ &\sim \frac{L}{\rho}2b_1\tau^2\frac{c_2^3}{a_2^3}\delta^{-5/2}\varepsilon\pi\frac{\sqrt{3}}{4}\Phi(0) \\ &\sim \frac{L}{\rho}b_1\frac{c_2a_2}{b_2^2}\delta^{-5/2}\varepsilon\pi\frac{9\sqrt{3}}{512}\Phi(0) \end{aligned}$$

so that the eigenvalue problem becomes

$$\lambda_0\Phi = \Phi_{yy} + (-1+2w)\,\Phi - \chi\Phi(0), \tag{3.6}$$

where

$$\begin{aligned} \lambda_0 &\equiv \lambda\frac{2}{a_2}, \\ \chi &\sim \frac{L}{\rho}c_2\frac{b_1}{b_2}\delta^{-5/2}\varepsilon\pi\frac{9\sqrt{3}}{256}. \end{aligned}$$

Simplifying further, we get that $\chi = \chi_b$, where

$$\chi_b = \frac{\varepsilon^{-2/3}}{4\rho}\left(4\frac{a_1}{a_2} - \frac{b_1}{b_2} - 3\frac{c_1}{c_2}\right)^{5/3} c_2\left(\frac{b_1}{b_2}\frac{\pi}{2}\right)^{-2/3} L^{8/3}. \tag{3.7}$$

In particular, $\chi_b = O(1)$ when $\rho = O(\varepsilon^{-2/3})$.

For the even eigenvalue $\psi'(L) = 0$, the analysis is similar to the previous construction; the reduced problem is still (3.6) but with

$$\chi = O\left(\varepsilon^{-2/3}\right) \gg 1.$$

Stability of K interior spikes. We now modify the computation above to the case of K spikes. We follow the methods used in [4] and [19]. We first consider the linearized problem (3.1), (3.2) with K spikes on the interval $[-L, (2K-1)L]$ and with *periodic boundary conditions*

$$\begin{aligned} &\phi(-L) = \phi((2K-1)L), \quad \phi'(-L) = \phi'((2K-1)L), \\ &\psi(-L) = \psi((2K-1)L), \quad \psi'(-L) = \psi'((2K-1)L). \end{aligned} \tag{3.8}$$

To solve this, first consider the following boundary conditions on $[-L, L]$:

$$\phi(L) = z\phi(-L), \quad \phi'(L) = z\phi'(-L), \tag{3.9}$$

$$\psi(L) = z\psi(-L), \quad \psi'(L) = z\psi'(-L), \tag{3.10}$$

where z is a parameter to be chosen later; then we extend ψ, ϕ to the whole interval $[-L, (2K-1)L]$ by imposing continuity at $L, 3L, \ldots$ of ϕ, ψ and their first derivative. It then follows that $\phi((2K-1)L) = z^K\phi(-L)$, etc. Therefore (3.9) are equivalent to (3.8), whenever $z^K = 1$ or

$$z = \exp(i\theta), \quad \theta = \frac{2\pi k}{K}, \quad k = 0, \ldots, K-1. \tag{3.11}$$

The outer problem is, as before, $\psi_{xx} = 0$, but the boundary conditions are now given by (3.10). Similarly to previous computation, we choose a number $\sigma^+ > 0$ with $\varepsilon\delta^{1/2} \ll \sigma^+ \ll \varepsilon$ and another number $\sigma^- < 0$ with $\varepsilon\delta^{1/2} \ll -\sigma^- \ll \varepsilon$ and integrate (3.2) on the interval $[\sigma^-, \sigma^+]$. We then obtain, to leading order,

$$\rho\left[\psi'(\sigma^+) - \psi'\left(\sigma^-\right)\right] + 2b_1\tau^2\int_{\sigma^-}^{\sigma^+}\frac{\phi}{v^3} \sim 0,$$

where we simplify as before,

$$\int_{\sigma^-}^{\sigma^+}\frac{\phi}{v^3} \sim \frac{c_2^3}{a_2^3}\delta^{-5/2}\varepsilon\pi\frac{\sqrt{3}}{2}\Phi(0).$$

Therefore we may write

$$\psi(x) = \left(-\frac{2b_1\tau^2}{\rho}\frac{c_2^3}{a_2^3}\delta^{-5/2}\varepsilon\pi\frac{\sqrt{3}}{2}\Phi(0)\right)\eta(x),$$

where $\eta(x)$ solves

$$\begin{cases} \eta_{xx} = 0, \\ \eta_x(0^+) - \eta_x(0^-) = 1, \quad \eta(0^+) = \eta(0^-), \\ \eta(L) = z\eta(-L), \quad z = \exp(i\theta). \end{cases} \tag{3.12}$$

To satisfy the boundary conditions, we must have

$$\eta(x) = \begin{cases} Ax + B, & x < 0, \\ z\,(Ax + B - 2AL)\,, & x > 0. \end{cases}$$

Imposing the jump conditions we obtain

$$(z-1)\,A = 1, \qquad B = z\,(B - 2AL)\,.$$

We compute

$$B = 2AL\frac{z}{z-1}, \qquad A = \frac{z-1}{(z-1)^2}$$

so that

$$\eta(0) = B = \frac{2Lz}{(z-1)^2}.$$

Note that $\frac{(z-1)^2}{z} = z + \bar{z} - 2 = 2\,(\cos\theta - 1)$ so that

$$\eta(0) = \frac{L}{(\cos\theta - 1)}.$$

Therefore we obtain the problem (4.1), but with χ in (3.6) given by

$$\chi_\theta = \frac{2}{1-\cos\theta}\chi_b, \tag{3.13}$$

where χ_b is given by (3.7).

Finally, we show that the stability of a K spike pattern with Neumann boundary conditions can be derived from the stability of a $2K$ spike pattern with periodic boundary conditions. Suppose that ϕ is a Neumann eigenfunction on the interval $[0, a]$. Extend it by an even reflection around zero to an eigenfunction on the interval of size $[-a, a]$. Such an extension then satisfies periodic boundary conditions on $[-a, a]$. It follows that the Neumann spectrum of K spikes is a subset of a periodic spectrum of $2K$ spikes. On the other hand, if ϕ is a periodic eigenfunction on $[-a, a]$, then define $\hat{\phi}(x) = \phi(x) + \phi(-x)$. Then $\hat{\phi}$ is a Neumann eigenfunction on $[0, a]$, provided that $\hat{\phi}$ is not identically zero. Since $\hat{\phi}'(0) = 0$, this is equivalent to $\hat{\phi}\,(0) \neq 0$ or $\phi\,(0) \neq 0$. A direct verification shows that this corresponds to choosing θ in (3.13) to be one of

$$\theta = \frac{\pi k}{K}, \quad k = 0, \ldots, K-1.$$

Moreover (3.13) attains its minimum when $k = K - 1$; this is the first unstable mode as ρ is increased.

The stability of large eigenvalues now reduces to the study of the reduced problem (3.6), which is the topic of the next section. It is found that (3.6) is stable for $\chi > \chi_c = 0.669$ and is unstable otherwise. This completes the analysis of the large eigenvalues and the derivation of the thresholds (1.6), (1.7).

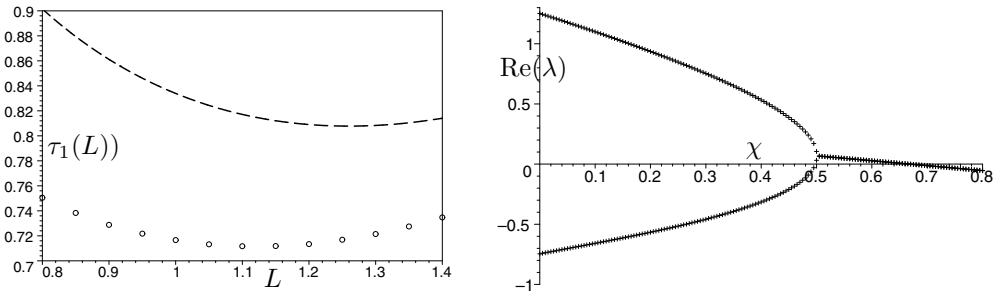

FIG. 3. (a) *The graph of the function* $L \to \tau_1(L)$ *(see section* 5*). Full numerics are shown by circles; the dashed line shows the asymptotics. See Experiment* 2 *of section* 7 *for details and parameter values.* (b) *Bifurcation diagram for the problem* (4.1)*. A Hopf bifurcation occurs at* $\chi = \chi_c = 0.669$*. For* $\chi < \chi_c$*, the problem is unstable. It becomes stable for* $\chi > \chi_c$*.*

4. Reduced eigenvalue problem. We now turn to the analysis of the reduced problem for the large eigenvalues:

$$\begin{cases} \lambda\Phi = \Phi_{yy} + (-1 + 2w)\,\Phi - \chi\Phi(0), \\ \Phi \text{ is even and is bounded as } |y| \to \infty. \end{cases} \tag{4.1}$$

This is a novel problem which we will call the *point-weight eigenvalue problem (PWEP).* See the discussion in section 8 for related nonlocal eigenvalue problems (NLEPs) that occur in many other reaction-diffusion systems. We show the following two results.

PROPOSITION 4.1. *The point spectrum to* (4.1) *can be written implicitly in terms of hypergeometric functions as the solution to the following transcendental equation for* λ*:*

$$\lambda = -1 - \chi + 2\chi\Phi_0(0), \tag{4.2}$$

where

$$\Phi_0(0) = \frac{6\pi\lambda\,(\lambda+1)}{\sin(\pi\alpha)\,(4\lambda-5)\,(4\lambda+3)} - \frac{3}{2\lambda}\left\{ {}_3F_2\left(\begin{array}{c} 1, 3, -1/2 \\ 2+\alpha,\ 2-\alpha \end{array} ; 1 \right) \right\} \tag{4.3}$$

and

$$\alpha = \sqrt{1+\lambda}. \tag{4.4}$$

Using Proposition 4.1, we can numerically compute the bifurcation diagram. We used Maple to evaluate (4.3) numerically. Figure 3 shows the resulting bifurcation diagram. When $\chi = 0$, (4.1) admits two eigenvalues, $\lambda = 5/4$ and $\lambda = -3/4$ (see, for example, [10]). Also when $\chi = \frac{1}{2}$, the negative eigenvalue crosses through zero. Shortly thereafter the eigenvalues become complex-valued, and eventually stability is achieved through a Hopf bifurcation at $\chi = \chi_c = 0.669$; see Figure 3(b). Let us summarize these observations as follows.

PRINCIPAL RESULT 4.2. *Suppose that* $\chi < \frac{1}{2}$*. Then the problem* (4.1) *admits a strictly positive eigenvalue. On the other hand, there exists a number* χ_c *such that all eigenvalues* λ *of* (4.1) *have negative real parts whenever* $\chi > \chi_c$*. Numerically, we find that* $\chi_c = 0.669$*.*

The derivation of instability for $\chi < \frac{1}{2}$ is done rigorously below. To show stability, we make use of a winding number argument similar to that in [21]. However, the final part of our argument relies on a numerical computation, as will be shown below. Unlike the related NLEP (8.5), a fully rigorous proof of the stability of NWEP (4.1) is still an open question; see section 8.

Proof of Proposition 4.1. We decompose $\Phi(y) = \Phi^\star + \Phi_0(y)$ such that $\Phi^\star$ is a constant and $\Phi_0 \to 0$ as $|y| \to \infty$. Substituting $\Phi(y) = \Phi^\star + \Phi_0(y)$ into (4.1), we find that $\lambda\Phi^\star = -\Phi^\star - \chi\left(\Phi_0(0) + \Phi^\star\right)$ and that Φ_0 satisfies $\lambda_0\Phi_0 = \Phi_{0yy} - \Phi_0 + 2w\Phi_0 + 2w\Phi^\star$. We then obtain $\Phi^\star = -\chi\Phi_0(0)/(\chi+\lambda+1)$, so that the problem (4.1) becomes

$$\lambda_0\Phi_0 = \Phi_{0yy} - \Phi_0 + 2w\Phi_0 - \frac{2\chi}{\chi+\lambda+1}\Phi_0(0)w. \tag{4.5}$$

We also scale $\Phi(y)$ so that $\frac{2\chi}{\chi+\lambda+1}\Phi_0(0) = 1$; the problem (4.5) then becomes

$$\begin{cases} \Phi_{0yy} - \alpha^2\Phi_0 + 2w\Phi_0 = w, \\ \lambda = -1 - \chi\left(1 - 2\Phi_0(0)\right), \\ \alpha = \sqrt{1+\lambda}, \end{cases} \tag{4.6}$$

where we take the branch of the root so that $\mathrm{Re}(\alpha) \geq 0$. Next, we will use hypergeometric functions to study (4.6).

We make a change of variables

$$\Phi_0 = w^\alpha G$$

to get

$$G_{yy} + 2\alpha\frac{w'}{w}G' + wG\left\{2 - \frac{2}{3}\alpha^2 - \frac{1}{3}\alpha\right\} = w^{1-\alpha}.$$

Next we make a change of dependent variables; let

$$z = \frac{2}{3}w(y).$$

Note that $z(y)$ is one-to-one with $z \to 0$ as $y \to \infty$ and $z \to 1$ as $y \to 0$. Using the identity

$$w'^2 = w^2 - \frac{2}{3}w^3,$$

we then obtain

$$\begin{gathered} z(1-z)G_{zz} + \left(c - (a+b+1)\,z\right)G_z - abG = \left(\tfrac{3}{2}\right)^{1-\alpha} z^{-\alpha}; \\ \text{with} \quad c := 1 + 2\alpha; \quad a := 2 + \alpha; \quad b := \alpha - \tfrac{3}{2}. \end{gathered} \tag{4.7}$$

This is a hypergeometric ODE with an inhomogeneity. To study (4.7), we proceed as in [24]; see also [19]. To determine a particular solution, we seek the series solution of the form

$$G_p = z^s \sum_0^\infty c_k z^k.$$

We then determine that

$$s = 1-\alpha;$$
$$c_0 = \left(\frac{3}{2}\right)^{1-\alpha}\frac{1}{1-\alpha^2};$$
$$c_k = \frac{(k+2)\left(k-\frac{3}{2}\right)}{(k+1+\alpha)(k+1-\alpha)}c_{k-1}, \quad k \geq 1.$$

Therefore G_p can be written as

$$G_p = \left(\frac{3}{2}\right)^{1-\alpha}\frac{1}{1-\alpha^2}z^{1-\alpha}{}_3F_2\left(\begin{array}{c} 1,3,-1/2 \\ 2+\alpha,\ 2-\alpha \end{array};z\right).$$

Recalling that a homogeneous solution to (4.7) is given by

$$G_h = A_1{}_2F_1\left(\begin{array}{c} a,b \\ c \end{array};z\right) + A_2 z^{1-c}{}_2F_1\left(\begin{array}{c} b-c-1, a-c+1 \\ 2-c \end{array};z\right),$$

we then obtain that

$$\Phi_0(y) = B_1 z^{\alpha}{}_2F_1\left(\begin{array}{c} 2+\alpha,\ \alpha-3/2 \\ 1+2\alpha \end{array};z\right) + B_2 z^{-\alpha}{}_2F_1\left(\begin{array}{c} -\alpha-3/2,\ 1-\alpha \\ 1-2\alpha \end{array};z\right),$$
$$+\frac{3}{2}\frac{1}{1-\alpha^2}z{}_3F_2\left(\begin{array}{c} 1,3,-1/2 \\ 2+\alpha,\ 2-\alpha \end{array};z\right),$$

where the constants B_1 and B_2 are to be determined. First note that $B_2 = 0$, since $\Phi_0(\infty)$ is finite. Next we outline the determination of B_1, which will be chosen to satisfy $\Phi_0'(0) = 0$. Note that

$$\frac{d\phi}{dy} = \frac{d\phi}{dz}z(1-z)^{1/2},$$

and let

$$f(z) = {}_3F_2\left(\begin{array}{c} 1,3,-1/2 \\ 2+\alpha,\ 2-\alpha \end{array};z\right).$$

Written explicitly, we have

$$f(z) = c_0 + c_1 z + c_2 z^2 + \cdots,$$

where

$$c_0 = 1, \quad c_k = \frac{(k+2)(k-3/2)}{(k+1-\alpha)(k+1+\alpha)}c_{k-1}, \quad k \geq 1.$$

Expanding for large k, we note that

$$\frac{(k+2)(k-3/2)}{(k+1-\alpha)(k+1+\alpha)} \sim 1 - \frac{3}{2}\frac{1}{k} \quad \text{as } k \to \infty$$

so that

$$c_k \sim \prod_{j=1}^{k}\left(1-\frac{3}{2}\frac{1}{j}\right) \sim \exp\left\{\sum^{k}\ln\left(1-\frac{3}{2}\frac{1}{j}\right)\right\}$$
$$\sim \exp\left\{-\frac{3}{2}\sum^{k}\frac{1}{j}\right\} \sim \frac{\hat{c}}{k^{3/2}} \quad \text{as } k\to\infty,$$

where

$$\hat{c} = \lim_{K\to\infty} K^{3/2}\prod_{k=1}^{K}\frac{(k+2)\,(k-3/2)}{(k+1-\alpha)\,(k+1+\alpha)}.$$

In particular, for $z\to 1$, the sum for $f(z)$ behaves like

$$f(z) \sim \hat{c}\sum^{\infty}\frac{z^n}{n^{3/2}} + C_0 + O(1-z) \quad \text{as } z\to 1,$$

where C_0 is some constant independent of z. Note that

$$f'(z) \sim \hat{c}\sum^{\infty}\frac{z^{n-1}}{n^{1/2}} \quad \text{as } z\to 1$$

so that $f'(z)\to\infty$ as $z\to 1$. However, the limit $\lim_{z\to 1} f'(z)\,(1-z)^{1/2}$ turns out to be finite, as we now compute. Consider

$$u(h) = \sum^{\infty}\frac{(1-h)^{n-1}}{n^{1/2}}h^{1/2}.$$

In the limit $h\to 0$, we estimate

$$u(h) \sim \sum^{\infty}\frac{\exp(-nh)}{n^{1/2}}h^{1/2} \sim \int_0^{\infty}\frac{\exp(-ht)}{\sqrt{t}}\sqrt{h}dt$$
$$\sim \int_0^{\infty} 2\exp\left(-s^2\right)ds \sim \sqrt{\pi} \quad \text{as } h\to 0.$$

Thus

$$\lim_{z\to 1} f'(z)\,(1-z)^{1/2} = \hat{c}\sqrt{\pi}.$$

Similarly, we let

$$g(z) = {}_2F_1\left(\begin{array}{c} 2+\alpha,\ \alpha-3/2 \\ 1+2\alpha \end{array};z\right),$$

and as with $f(z)$, we find that

$$\lim_{z\to 1} g'(z)\,(1-z)^{1/2} = \hat{d}\sqrt{\pi},$$

where

$$\hat{d} = \lim_{K\to\infty} K^{3/2}\prod_{k=1}^{K}\frac{(k+1+\alpha)\left(k+\alpha-\frac{5}{2}\right)}{(k+2\alpha)\,k}.$$

Therefore we obtain

$$\Phi_0'(0) = B_1\hat{d}\sqrt{\pi} + \frac{3}{2}\frac{1}{1-\alpha^2}\hat{c}\sqrt{\pi} = 0,$$

which yields

$$B_1 = \frac{-3}{2}\frac{1}{1-\alpha^2}\prod_{k=1}^{\infty}\frac{(k+2)\left(k-\frac{3}{2}\right)(k+2\alpha)\,k}{(k+1+\alpha)(k+1+\alpha)\left(k+\alpha-\frac{5}{2}\right)(k+1-\alpha)}.$$

Next we make use of the identity

$$\prod_{k=0}^{\infty}\frac{(k+a-b)(k+b+c)}{(k+a+d)(k+c-d)} = \frac{\Gamma(a+d)\,\Gamma(c-d)}{\Gamma(a-b)\,\Gamma(b+c)} \tag{4.8}$$

to simplify B_1 further. Using (4.8) we find that

$$\prod_{k=1}^{\infty}\frac{(k+2)(k+2\alpha)}{(k+1+\alpha)(k+1+\alpha)} = \prod_{k=0}^{\infty}\frac{(k+3)(k+1+2\alpha)}{(k+2+\alpha)(k+2+\alpha)} = \frac{\Gamma(2+\alpha)\,\Gamma(2+\alpha)}{\Gamma(3)\,\Gamma(1+2\alpha)},$$

$$\prod_{k=1}^{\infty}\frac{\left(k-\frac{3}{2}\right)k}{\left(k+\alpha-\frac{5}{2}\right)(k+1-\alpha)} = \prod_{k=0}^{\infty}\frac{\left(k-\frac{1}{2}\right)(k+1)}{\left(k+\alpha-\frac{3}{2}\right)(k+2-\alpha)} = \frac{\Gamma\left(\alpha-\frac{3}{2}\right)\Gamma(2-\alpha)}{\Gamma\left(-\frac{1}{2}\right)\Gamma(1)}$$

so that

$$B_1 = \frac{-3}{2}\frac{1}{1-\alpha^2}\frac{\Gamma(2+\alpha)\,\Gamma(2+\alpha)}{\Gamma(3)\,\Gamma(1+2\alpha)}\frac{\Gamma\left(\alpha-\frac{3}{2}\right)\Gamma(2-\alpha)}{\Gamma\left(-\frac{1}{2}\right)\Gamma(1)}.$$

We then use the standard identities

$$\Gamma(1-z)\,\Gamma(z) = \frac{\pi}{\sin(\pi z)}, \quad \Gamma(2z) = \Gamma(z)\Gamma\left(z+\frac{1}{2}\right)2^{2z-1}\pi^{-1/2}; \quad \Gamma\left(\frac{1}{2}\right) = \sqrt{\pi},$$

$${}_2F_1\left(\begin{array}{c} a,b \\ c \end{array};1\right) = \frac{\Gamma(c)\,\Gamma(c-a-b)}{\Gamma(c-a)\,\Gamma(c-b)}$$

to arrive at the formula (4.3). ∎

Derivation of Principal Result 4.2. We define

$$L_0\Phi := \Phi_{yy} + (-1+2w)\,\Phi \tag{4.9}$$

so that (4.5) can be written as

$$(L_0-\lambda)\Phi_0 = \Phi_0(0)\frac{2\chi}{\chi+1+\lambda}w. \tag{4.10}$$

Now note that $L_0(w+\frac{1}{2}yw_y) = w$, and if we take $\Phi_0 = w+\frac{1}{2}yw_y$, then $\Phi_0(0) = \frac{3}{2}$ so that (4.10) would be satisfied with $\lambda = 0$ and $\chi = 1/2$. We now show that for $\chi \in [0, \frac{1}{2})$, there is a strictly positive eigenvalue to (4.10). Define $\rho(\lambda)$ to be

$$\rho(\lambda) := \Phi_0(0), \quad \text{where } \Phi_0 = (L_0-\lambda)^{-1}w. \tag{4.11}$$

Then (4.10) is equivalent to solving

$$\rho(\lambda) = \frac{1+\lambda+\chi}{2\chi}. \tag{4.12}$$

We note that $L_0^{-1}w = w + \frac{1}{2}yw_y$ so that

$$\rho(0) = \frac{3}{2}. \tag{4.13}$$

On the other hand, $\rho(\lambda)$ has a vertical asymptote at the eigenvalue $\lambda = \lambda_0 = 5/4$ of the local operator L_0. To determine the behavior of $\rho(\lambda)$ near λ_0, we expand λ and ϕ near λ_0 as

$$\lambda = \lambda_0 + \delta, \quad \Phi_0 = \frac{a}{\delta}\phi_0 + \phi_1 + \cdots; \quad \delta \ll 1, \tag{4.14}$$

where ϕ_0 is the eigenfunction of the local operator L_0 satisfying $(L_0 - \lambda_0)\phi_0 = 0$ and where a is an $O(1)$ constant to be determined. We then obtain

$$(L_0 - \lambda_0)\phi_1 = a\phi_0 + w + O(\delta).$$

Multiplying both sides by ϕ_0 and integrating yields

$$a = -\frac{\int w\phi_0}{\int \phi_0^2} < 0.$$

Therefore we obtain

$$\rho(\lambda_0 + \delta) \sim -\frac{\int w\phi_0}{\int \phi_0^2}\phi_0(0)\frac{1}{\delta} + O(1) \quad \text{as} \quad \delta \to 0. \tag{4.15}$$

In particular,

$$\rho\,(\lambda) \to +\infty \quad \text{as} \quad \lambda \to \lambda_0^-. \tag{4.16}$$

By the intermediate value theorem, it follows from (4.16), (4.13) that (4.12) admits a solution $\lambda > 0$ whenever $0 \le \chi < \frac{1}{2}$.

To show stability of (4.1) for large χ, we first claim that $\operatorname{Re}\lambda \le C$ for some constant C independent of χ. Otherwise, there exists a sequence χ_k, λ_k with $|\lambda_k| \to \infty$ as $k \to \infty$ and with χ_k, λ_k being a solution to (4.5). But then $\frac{2\chi_k}{1+\lambda_k+\chi_k} \to 0$, and (4.5) becomes $\lambda_k\phi \sim L_0\phi$. However, this problem has bounded eigenvalues, contradicting $\lambda_k \to \infty$.

Since $|\lambda| < C$, we may take the limit $\chi \to \infty$; we then obtain

$$\begin{cases} \lambda\Phi_0 = \Phi_{0yy} + (-1 + 2w)\,\Phi_0 - 2\Phi_0(0)w, \\ \quad \Phi_0 \text{ is even and decays as } |y| \to \infty. \end{cases} \tag{4.17}$$

This problem is equivalent to solving

$$\rho(\lambda) - \frac{1}{2} = 0. \tag{4.18}$$

To determine the number of roots of (4.18), we will compute the winding number along an oriented contour C that consists of the semicircle $C_2 = R\exp(i\theta)$, $\theta = [-\pi/2, \pi/2]$, and segment $C_1 = [iR, -iR]$ along the imaginary axis traversed downwards. Taking the limit $R \to \infty$ yields the right half-plane.

Note that the solution to $(L_0 - \lambda)\Phi_0 = w$ has the asymptotics $\Phi_0 \sim w/\lambda$ for $|\lambda| \gg 0$, so that along the semicircle $|\lambda| = R \gg 1$, we have $\rho(\lambda) \sim \frac{3}{2R}\exp(-i\theta)$; it follows that $\Delta \arg_{C_1}\left[\rho - \frac{1}{2}\right] = 0$. To compute $\Delta \arg_{C_2}\rho$ consider the functions

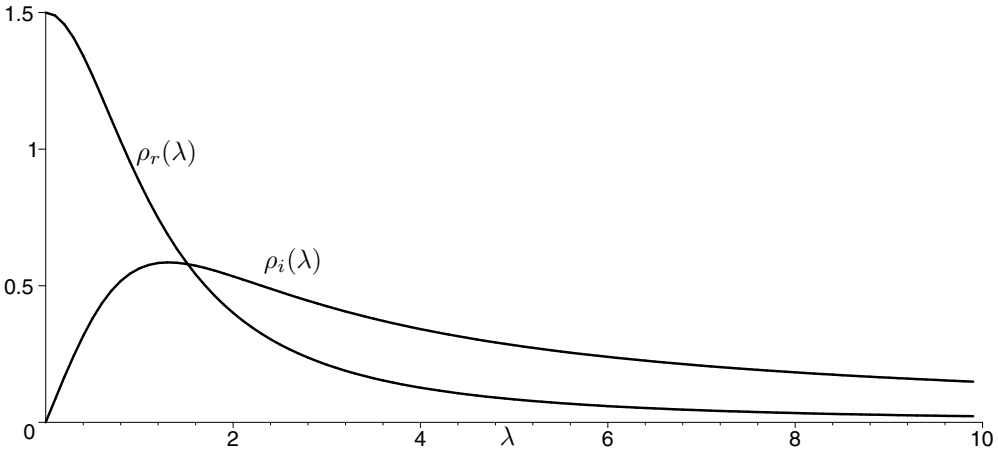

FIG. 4. *Graphs of* $\rho_r(\lambda)$ *and* $\rho_i(\lambda)$.

$\rho_R(t) = \operatorname{Re}\rho(it)$ and $\rho_I(t) = \operatorname{Im}\rho(it)$ with $t > 0$. Using Proposition 4.1, we computed their graphs as shown in Figure 4. We make the following observations:

$$\rho_R(0) - 1/2 = 1 \text{ and } \rho_R(t) - 1/2 \to -1/2 \text{ as } t \to \infty, \tag{4.19}$$

$$\rho_I(0) = 0,\ \rho_I(t) \to 0 \text{ as } t \to 0 \quad \text{and} \quad \rho_I(t) > 0 \text{ for } t > 0. \tag{4.20}$$

The asymptotics at $t = \infty$ and 0 are easily proved; on the other hand, *the positivity of* ρ_I *must be verified numerically.* From (4.19) and (4.20) it follows that the change in argument as $\rho(t) - \frac{1}{2}$ is traversed from $t = +i\infty$ to $t = 0$ is $-\pi$; by symmetry, $\Delta \arg_{C_1} \rho = -2\pi$ as $R \to \infty$, and $\Delta \arg_C \rho = -2\pi = 2\pi\,(N - S)$ where N is the number of zeros of ρ inside C and S is the number of singularities, counted with multiplicities. Note that $\rho(\lambda)$ is singular whenever λ is the eigenvalue of L_0 corresponding to an even eigenfunction; since L_0 has one such positive eigenvalue, we conclude that $S = 1$, and thus $N = 0$. This shows the absence of positive eigenvalues of (4.17), so that (4.1) is stable for sufficiently large χ. □

5. Small eigenvalues via asymmetric patterns. We now study the small eigenvalues. Rather than directly computing them, we first construct asymmetric patterns, and then compute the parameter value at which the asymmetric patterns bifurcate from the symmetric steady state. For the classical GM system, it was observed in [22] that such bifurcation corresponds precisely to the instability thresholds for the small eigenvalues; a similar structure was found to exist in for general reaction-diffusion systems that admit interface solutions [14]. Based on numerical evidence it appears that this correspondence also occurs for (1.2).

To construct an asymmetric pattern, we first consider a half-spike at the origin on the domain $[0, L]$. It will be confirmed later that the critical scaling is $\rho = O(\varepsilon^{-2/3})$. We therefore expand the outer region as

$$\rho = \rho_0 \varepsilon^{-2/3}, \tag{5.1}$$

$$\tau = \tau_0 + \varepsilon^{2/3}\tau_1 + \cdots, \qquad v = v_0 + \cdots, \tag{5.2}$$

where τ_0 is given by (2.7). In the outer region we get

$$\tau_{1xx} = g,$$

where

$$g = \frac{1}{\rho_0}\left(-\frac{\tau_0 a_1}{v_0} + \frac{\tau_0^2 b_1}{v_0^2} + \tau_0 c_1\right).$$

We recall (see Proposition 2.1) that in the outer region,

$$v_0 = \frac{3a_2}{4c_2}, \qquad \tau = \frac{3}{16}\frac{a_2^2}{b_2 c_2}$$

so that

$$g \sim \frac{1}{\rho_0}\frac{a_2^2}{4b_2}\left(-\frac{a_1}{a_2} + \frac{b_1}{4b_2} + \frac{3}{4}\frac{c_1}{c_2}\right),$$

$$\tau_1 = \tau_1(0) + \frac{(x-L)^2 - L^2}{2} g. \tag{5.3}$$

On the other hand, matching the inner and outer regions, we see that $\tau_1(0)$ is given by (2.28). Therefore we obtain

(5.4)

$$\tau_1(L) = L^{-2/3}\frac{3}{16}\frac{a_2^2}{b_2 c_2}\left(\frac{b_1}{b_2}\frac{\pi}{2}\right)^{2/3}\left(4\frac{a_1}{a_2} - \frac{b_1}{b_2} - 3\frac{c_1}{c_2}\right)^{-2/3} + L^2\frac{1}{\rho_0}\frac{a_2^2}{32b_2}\left(4\frac{a_1}{a_2} - \frac{b_1}{b_2} - 3\frac{c_1}{c_2}\right).$$

Note that the function $L \to \tau_1(L)$ is convex, with $\tau_1 \to \infty$ as $L \to 0$ or $L \to \infty$, and it attains a minimum when

$$\rho_0 = L^{8/3}\frac{c_2}{2}\left(\frac{b_1}{b_2}\frac{\pi}{2}\right)^{-2/3}\left(4\frac{a_1}{a_2} - \frac{b_1}{b_2} - 3\frac{c_1}{c_2}\right)^{5/3}. \tag{5.5}$$

(See Experiment 2 in section 7 and Figure 3(a) for an example and a comparison with full numerics.) This corresponds precisely to the bifurcation point: for values of ρ_0 above (5.5), an asymmetric solution can be constructed, whereas for ρ_0 below (5.5), only a symmetric branch can exist. The value of $\rho_{K,small}$ in (1.5) is then derived by substituting (5.5) into (5.1). This completes the derivation of Principal Result 1.1.

6. Construction of a spike in two dimensions. We now mimic the one-dimensional spike computations of section 2 to derive the asymptotics of the radially symmetric spike in two dimensions. As in section 2, we introduce

$$\tau = uv$$

to obtain the steady state problem for $\tau(x), v(x)$,

$$0 = d\Delta v + a_2 v - b_2\tau - c_2 v^2, \tag{6.1}$$

$$0 = \rho\Delta\tau + \tau\left(\frac{a_1}{v} - b_1\frac{\tau}{v^2} - c_1\right). \tag{6.2}$$

We seek steady state solutions with Neumann boundary conditions inside a radially symmetric domain Ω with a spike at the origin and $\rho \gg 1$, $d \ll 1$. To leading order, $\tau = \tau_0$ is constant, and we have the integral constraint

$$|\Omega|\, c_1 = \int_\Omega \left(\frac{a_1}{v} - b_1\frac{\tau_0}{v^2}\right). \tag{6.3}$$

As in section 2, we seek solutions for $v(x)$ in the form of an inverted spike so that $v(0)$ is very close to zero. We start with the standard spike ground state in two dimensions, which satisfies

$$\Delta w - w + w^2 = 0, \quad w \to 0 \text{ as } |y| \to \infty, \quad \max w = w(0),$$

and define

$$m := \max w(y) = w(0).$$

Making a change of variables

$$V_0(y) := m - w(y)$$

we obtain

$$\Delta V_0 + (2m-1)\, V_0 - V_0^2 - m\,(m-1) = 0. \tag{6.4}$$

In the inner region we transform

$$v\,(x) = \alpha V(y), \qquad x = \varepsilon y,$$

where the constants α and ε are to be specified later; then (6.1) becomes

$$0 = \Delta_y V + \frac{\varepsilon^2 a_2}{d} V - \frac{\varepsilon^2 b_2 \tau}{d\alpha} - \frac{\varepsilon^2 c_2 \alpha}{d} V^2. \tag{6.5}$$

In the inner region, we expand as

$$V = V_0 + \varepsilon^p V_1 + \cdots, \quad \tau = \tau_0 + \varepsilon^p \tau_1 + \cdots, \tag{6.6}$$

where the power $p > 0$ is to be determined; we then choose $\tau_0, \varepsilon\ \alpha$ so that the leading order of (6.5) becomes (6.4); that is,

$$\varepsilon = \sqrt{\frac{(2m-1)d}{a_2}}, \qquad \tau_0 = \frac{(m-1)m}{(2m-1)^2}\frac{a_2^2}{b_2 c_2}, \quad \alpha = \frac{1}{2m-1}\frac{a_2}{c_2}.$$

Proceeding as in one dimension, at the next order we get $L_0 V_1 = \delta_0$ with $L_0 \Phi \equiv \Delta\Phi - \Phi + 2\Phi w$ and

$$\delta_0 \equiv \frac{b_2 c_2 (2m-1)^2}{a_2^2}\tau_1$$

so that, using the identities $L_0 1 = -1 + 2w$ and $L_0\left(\frac{y\cdot\nabla w}{2} + w\right) = w$, we obtain

$$V_1 = -\delta_0 + 2\delta_0\left(\frac{y\cdot\nabla w}{2} + w\right). \tag{6.7}$$

In summary, to two orders we have

$$V \sim m - w + \delta\,(2w - 1 + y\cdot\nabla w)\,, \qquad \delta \equiv \delta_0 \varepsilon^p = \frac{b_2 c_2 (2m-1)^2}{a_2^2}\tau_1 \varepsilon^p.$$

Next we expand for small y. Note that

$$w(y) \sim m - \frac{m(m-1)}{2} R^2, \quad R = |y| \ll 1,$$

so that

$$V(y) \sim \frac{m(m-1)}{2} R^2 + (2m-1)\,\delta, \quad R = |y| \ll 1,$$

and in the outer region we have

$$V \sim m, \quad |y| \gg 1.$$

Next we estimate $\int_\Omega \frac{1}{V^2}$. Write

$$\int_\Omega \frac{1}{V^2} \sim \int_{B_\gamma} \frac{1}{V^2} + \int_{\Omega \setminus B_\gamma} \frac{1}{V^2},$$

where B_γ is a disk of small radius γ to be specified later. We compute

$$\begin{aligned}
\int_{\Omega \setminus B_\gamma} \frac{1}{V^2} &\sim 2\pi\varepsilon^2 \int_0^{\frac{\gamma}{\varepsilon}} \frac{RdR}{(V(R))^2} \\
&\sim 2\pi \frac{\varepsilon^2}{\delta} \int_0^{\frac{\gamma}{\varepsilon\sqrt{\delta}}} \frac{sds}{\left(\frac{m(m-1)}{4} s^2 + (2m-1)\right)^2} \\
&\sim 2\pi \frac{\varepsilon^2}{\delta} \frac{16}{(m^2-m)^2} \int_0^\infty \frac{sds}{\left(s^2 + \frac{(2m-1)4}{m^2-m}\right)^2} \\
&\sim \frac{\varepsilon^2}{\delta} \frac{4\pi}{(m^2-m)\,(2m-1)}.
\end{aligned}$$

To balance other terms in (6.3), we will need to choose $\delta = O(\varepsilon^2)$ so that $p = 2$. On the other hand, for the computation above to be valid, we also assume that $\frac{\gamma}{\varepsilon\sqrt{\delta}} \gg 1$ and $\frac{\gamma}{\varepsilon} \ll 1$. These assumptions can be satisfied by choosing $\varepsilon^2 \ll \gamma \ll \varepsilon$, so that the approximation is self-consistent. We therefore obtain

$$\int_\Omega \frac{1}{V^2} \sim \frac{\varepsilon^2}{\delta} \frac{4\pi}{(m^2-m)\,(2m-1)} + \frac{|\Omega|}{m^2}. \tag{6.8}$$

A similar computation yields

$$\int_\Omega \frac{1}{V} \sim \frac{|\Omega|}{m} + o(1). \tag{6.9}$$

Substituting (6.8), (6.9) into (6.3) we get

$$|\Omega|\, c_1 \sim \frac{a_1 c_2}{a_2} \frac{(2m-1)\,|\Omega|}{m} - \frac{b_1 c_2}{b_2} \left(\frac{\varepsilon^2}{\delta} \frac{4\pi}{(2m-1)} + \frac{|\Omega|\,(m-1)}{m} \right),$$

$$\delta \sim \frac{\varepsilon^2}{|\Omega|} \frac{4\pi b_1 m}{b_2\,(2m-1)} \frac{1}{\left(\frac{a_1}{a_2}\,(2m-1) - (m-1)\,\frac{b_1}{b_2} - m\frac{c_1}{c_2} \right)}.$$

In summary, we obtain the following proposition.

PROPOSITION 6.1. *Consider the steady state equations*

$$0 = d\Delta v + a_2 v - b_2 uv - c_2 v^2, \qquad 0 = \rho\Delta\,(vu) + a_1 u - b_1 u^2 - c_1 uv \tag{6.10}$$

on a disk $\Omega \in \mathbb{R}^2$ centered at the origin with Neumann boundary conditions. Let w be the unique ground state solution of (2.14) *and define*

$$m = \max w \approx 2.39195.$$

Suppose that

$$\frac{a_1}{a_2}(2m-1) - (m-1)\frac{b_1}{b_2} - m\frac{c_1}{c_2} > 0 \tag{6.11}$$

and consider the asymptotic limit

$$d \ll 1, \quad \rho \gg 1. \tag{6.12}$$

The system (6.10) *admits a solution such that $v(x)$ has the form of an inverted spike at $x = 0$, with its minimum close to zero. More precisely, we have*

$$v(x) \sim \frac{1}{2m-1}\frac{a_2}{c_2}\left(m - w(R) + \delta\left(2w(R) - 1 + Rw'(R)\right)\right), \qquad R = \frac{|x|}{\varepsilon},$$
$$u \sim \frac{\tau_0}{v(x)},$$

where

$$\varepsilon := \sqrt{\frac{(2m-1)d}{a_2}}, \qquad \tau_0 := \frac{(m-1)m}{(2m-1)^2}\frac{a_2^2}{b_2 c_2}, \tag{6.13}$$

$$\delta \sim \frac{\varepsilon^2}{|\Omega|}\frac{4\pi b_1 m}{b_2(2m-1)}\frac{1}{\left(\frac{a_1}{a_2}(2m-1) - (m-1)\frac{b_1}{b_2} - m\frac{c_1}{c_2}\right)}. \tag{6.14}$$

In particular,

$$v(0) \sim \frac{a_2}{c_2}\delta, \quad u(0) \sim \frac{(m-1)m}{(2m-1)^2}\frac{a_2}{b_2}\frac{1}{\delta}. \tag{6.15}$$

7. Numerics. We turn to numerics to validate our asymptotic results. We have used the software FlexPDE [5] to perform the simulations of the full system (1.2). In one dimension, due to the peculiarity of the critical scaling $\rho = O(d^{-1/3})$, the error in asymptotic results can be seen to be of $O(d^{1/3})$. This means that generally an extremely small value of d is required to obtain a decent comparison with the asymptotic results.

Experiment 1: Steady state. We first consider a steady state consisting of a half-spike at the origin on $[0, L]$, as constructed in Proposition 2.1. In particular, we explore the expected error as a function of d. We recall from Proposition 2.1 the asymptotic formulae

$$v(0) \sim \left(\frac{\varepsilon}{L}\right)^{2/3}\frac{3}{4}\frac{a_2}{c_2}\left(\frac{b_1}{b_2}\frac{\pi}{2}\right)^{2/3}\left(4\frac{a_1}{a_2} - \frac{b_1}{b_2} - 3\frac{c_1}{c_2}\right)^{-2/3}, \tag{7.1}$$

$$u(0) \sim \left(\frac{\varepsilon}{L}\right)^{-2/3}\frac{1}{4}\frac{a_2}{b_2}\left(\frac{b_1}{b_2}\frac{\pi}{2}\right)^{-2/3}\left(4\frac{a_1}{a_2} - \frac{b_1}{b_2} - 3\frac{c_1}{c_2}\right)^{2/3}. \tag{7.2}$$

TABLE 1

d	$\varepsilon = \sqrt{2d/a_2}$	$u(0)$ from numerics	$u(0)$ from asymptotics (7.2)	%error= (col2-col3)/col3
10^{-1}	0.2	8.8078	4.8486	81.65%
10^{-2}	0.0632	14.6938	10.446	40.66%
10^{-3}	0.02	27.0225	22.505	20.07%
10^{-4}	0.0632	53.2865	48.486	9.90%
10^{-5}	0.002	109.634	104.46	4.95%

We take

$$L = 1, \rho = 200, \quad (a_1, b_1, c_1) = (5, 1, 1), \quad (a_2, b_2, c_2) = (5, 1, 5), \tag{7.3}$$

and we vary d. We then read off the numerically computed $u(0)$ and compare it the asymptotic result (7.2). Table 1 summarizes our results.

Note that decreasing d by a factor of 10^3 decreases the relative error by a factor of about 10. This demonstrates that, as expected, the error behaves like $O(d^{1/3})$. Also note that even with $d = 10^{-3}$, the error is about 20%. Therefore a very small value of d is required to obtain good agreement with numerics.

Experiment 2: Asymmetric states. We fix

$$d = 10^{-3}, \quad \rho = 200, \quad (a_1, b_1, c_1) = (5, 1, 1), \quad (a_2, b_2, c_2) = (5, 1, 5) \tag{7.4}$$

and numerically compute $\tau(L) = v(L)u(L)$ for several values of L. From $\tau(L)$, we then numerically compute $\tau_1(L) = [\tau(L) - \tau_0]\,\varepsilon^{-2/3}$, where τ_0 is given by (2.7). We then compare this computation with the asymptotic result for $\tau_1(L)$ as given by (5.4). The results are summarized in Table 2.

TABLE 2

L	$\tau_1(L)$ from numerics	$\tau_1(L)$ from asymptotics (5.4)
0.80	0.75054	0.9015
0.85	0.73832	0.87952
0.90	0.72882	0.8612
0.95	0.72176	0.84613
1.00	0.71661	0.83395
1.05	0.71321	0.82438
1.10	**0.71172**	0.81716
1.15	0.71186	0.81211
1.20	0.7134	0.80905
1.25	0.71693	**0.80784**
1.30	0.72149	0.80834
1.35	0.72752	0.81046
1.40	0.73479	0.8141

The graph of $\tau_1(L)$ is given in Figure 3(a). The instability threshold for the small eigenvalue corresponds to the minimizer of the function $L \to \tau(L)$, shown in bold in Table 2. Asymptotically, by solving (1.5) with $\rho_{K,small} = \rho$ for $L = L_{K,small}$ we obtain

$$L_{K,small} = 1.2598. \quad \text{[asymptotics]}$$

On the other hand, from Table 2, the minimum occurs at around

$$L_{K,small} = 1.1. \quad \text{[numerics]}$$

The relative error is about 15% and is of the same magnitude as the relative error in the steady state itself (see Experiment 1).

Experiment 3. We take parameter values as in (7.4) and vary K and L. First, consider the case of K interior spikes with $K = 2, 3$. Taking $L = 1.5$, we obtain from Principal Result 1.1 that $\rho_{2,small} = \rho_{3,small} = 318.5 > \rho$, $\rho_{2,large} = 476.1 > \rho$, and $\rho_{3,large} = 317.4 > \rho$. Therefore a pattern consisting of either two or three interior spikes is expected to be stable. This is indeed confirmed by direct numerical simulations. The case $K = 2$ is shown in Figure 2(a); the figure is similar for $K = 3$ (not shown).

Next, we take $L = 1$. We then compute $\rho_{2,small} = \rho_{3,small} = 108.0 < \rho$, $\rho_{2,large} = 161 < \rho$, $\rho_{3,large} = 108 < \rho$. Therefore either two or three interior spikes are unstable with respect to small and large eigenvalues. On the other hand, numerically, we observe that two interior spikes are stable with respect to large eigenvalues, whereas three interior spikes are unstable with respect to both small and large eigenvalues (Figure 2(b) and (d)): two spikes slowly drift away from their symmetric equilibria until one of them disappears, but only after a long time $t \sim 12000$, whereas three spikes are destabilized in $O(1)$ time and one of them disappears at $t \sim 20$.

The fact that two spikes are observed to be numerically stable with respect to large eigenvalues even though $\rho_{2,large} < \rho$ is not surprising since $\rho = 200$ and $\rho_{2,large} = 161$ is within 20% of ρ. This is within expected error range (see Experiment 2). As an additional test and to verify that this discrepancy is due to d being insufficiently small, we next decreased d by 10 so that $d = 10^{-4}$, while at the same time increasing ρ by $10^{1/3}$ so that $\rho = 200 \times 10^{1/3} = 430.88$. Keeping all other parameters as before, this preserves the critical scaling $\rho = O(d^{-1/3})$, and the predicted behavior for two spikes is the same as before, that is, unstable with respect to both large and small eigenvalues. Indeed, with the decreased d, fast-scale instability was observed with one of the spikes disappearing at $t \approx 20$. Moreover, $O(1)$ oscillations were observed before spike death; this confirms the fact that the instability of the large eigenvalue is due to a Hopf bifurcation.

Finally, consider the case of a double-boundary spike with $L = 1$. Then $\rho_b = 80.7 < \rho$ so that such a configuration is unstable with respect to large eigenvalues. This is indeed observed numerically as illustrated in Figure 2(c). On the other hand, if $L = 1.5$, then $\rho_b = 238 > \rho$ and the double-boundary configuration is predicted to be stable; we have verified numerically that this is indeed the case.

Experiment 4: $\rho = O(1)$. We explore numerically what happens when ρ is decreased. When $\rho = O(1)$, the outer region for τ is no longer nearly constant. Numerically, we observe *spike insertion* when ρ is sufficiently small: a spike appears when the distance between two spikes becomes too big; see Figure 5. With $\rho = 7$ and $d = 5 \times 10^{-4}$, peak insertion is observed. Similar complicated dynamics were observed when d was decreased to $d = 10^{-5}$ while keeping other parameters constant. Finally, we took $\rho = 20$ and varied d from 10^{-2} to 10^{-5}. No peak insertion was observed. This confirms that as expected, spike insertion is independent of d, i.e., it occurs when $\rho = O(1)$. A similar phenomenon was observed in the model of volume-filling chemotaxis [6]. A related phenomenon of self-replication is well known for other reaction-diffusion systems; see, for example, [9], [18]. It is possibly due to the disappearance of the solution in the outer region. A full explanation of this phenomenon is left for future work.

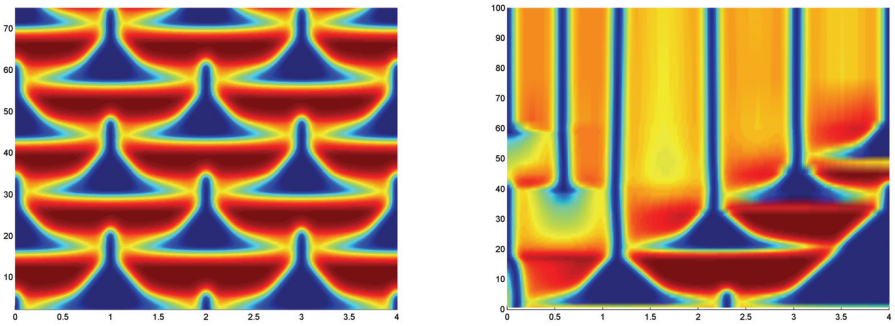

FIG. 5. *Sensitivity to initial conditions. The left and right figures differ only in the initial conditions. On the left, symmetric initial conditions result in an intricate time-periodic solution. On the right, the initial condition is the same as on the left, except for a shift of* 0.1 *units to the right. Dynamics eventually settle to a five-spike stable pattern. Parameter values for both figures are* $\rho = 7$, $d_2 = 0.0005$, $(a_1, b_1, c_1) = (5, 1, 1)$, *and* $(a_2, b_2, c_2) = (1, 1, 2)$.

TABLE 3

d	ε from (6.13)	δ from (6.14)	$u(0)$ from numerics	$u(0)$ using (6.15)	%er= (col4-col5)/col5
0.08	0.246	0.08	21.34	25.398	46.5%
0.04	0.173	0.04	37.00	29.067	27%
0.02	0.123	0.02	67.64	58.134	16.4%
0.01	0.0869	0.01	128.1	116.269	10.2%
0.005	0.0615	0.005	248.8	232.539	7%

Experiment 5: Two-dimensional steady state. We take the domain Ω to be the unit disk and compute the radially symmetric two-dimensional spike centered at the origin; we then read off $u(0)$ and compare with the analytical result of Proposition 6.1 We take

$$\rho = 50, \quad (a_1, b_1, c_1) = (5, 1, 1), \quad (a_2, b_2, c_2) = (5, 1, 5) \tag{7.5}$$

and vary d as in Table 3.

From Table 3, we note that decreasing d by a factor of 2 decreases the relative error by a factor of $2^{2/3}$. Hence the expected relative error is of $O(d^{2/3})$. Such error behavior is much better than the $O(d^{1/3})$ error that was observed in one dimension.

Experiment 6: Dynamics in two dimensions. We take the parameter values as in (7.5) except for ρ which we vary. A wide range of possible dynamical behavior is observed for different ranges of ρ; see Figure 6.

8. Discussion. The instability thresholds of Principal Result 1.1 are qualitatively similar to other reaction-diffusion models without cross-diffusion. One of the most well studied is the Gierer–Meinhardt (GM) system, whose stability was studied in great detail in [4] and [19]. To be concrete, consider the "standard" GM system,

$$a_t = \varepsilon^2 a_{xx} - a + a^2/h, \qquad 0 = Dh_{xx} - h + a^2. \tag{8.1}$$

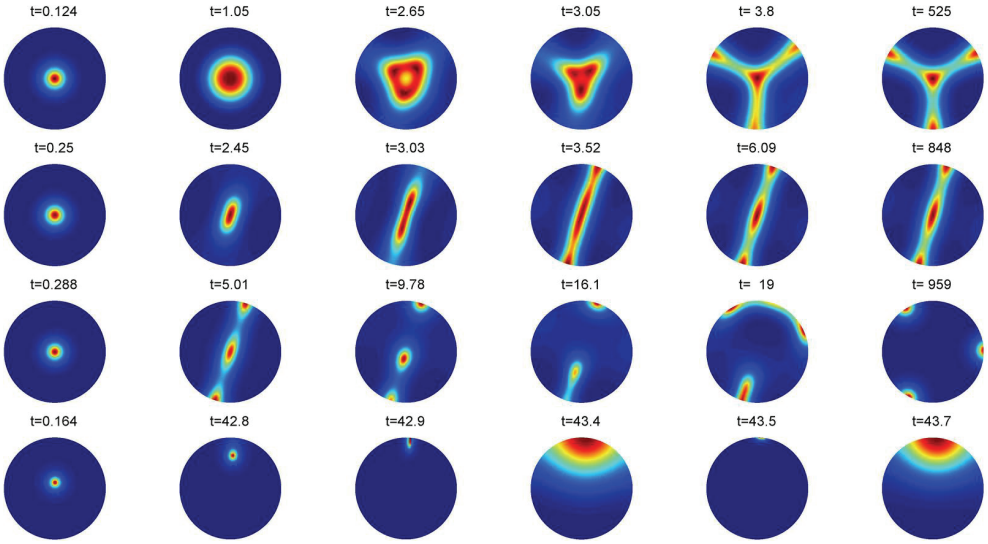

FIG. 6. *Various dynamics observed in a two-dimensional disk. Parameter values are as given by* (7.5) *except for* ρ *as specified below. Row* 1: $\rho = 2$. *Spot splits into three spots. Row* 2: $\rho = 4$. *Initially, spot splits into two, and the final steady state consists of two boundary spots and one center spot. Row* 3: $\rho = 6$. *Row* 4: $\rho = 500$. *The interior spike is unstable and slowly drifts to the boundary. Once it reaches the boundary, it starts to oscillate indefinitely.*

The steady state for the GM system considered in [4] consists of K *spikes*, concentrated at K symmetrically spaced points. The authors derived a sequence of thresholds

$$D_1^\star = \varepsilon^2 \exp(2/\varepsilon)/125, \tag{8.2}$$

$$D_K^\star = \frac{1}{\left[K \ln\left(\sqrt{2}+1\right)\right]^2}, \ K \geq 2, \tag{8.3}$$

such that K spikes on the interval $[-1,1]$ are stable if $D < D_K^\star$ and unstable if $D > D_K^\star$. Moreover, it was found that the instability is always triggered by small eigenvalues. By comparison, the stability thresholds for K spikes of (1.2) on the interval of length 2 (Principal Result 1.1 with $L = \frac{1}{K}$) become

$$\rho_{K,\text{small}} := \varepsilon^{-2/3} K^{-8/3} C_0, \qquad \rho_{K,\text{large}} := \rho_{K,\text{small}} \frac{1.494}{1-\cos\left[\pi\left(1-1/K\right)\right]}, \tag{8.4}$$

where $C_0 := \frac{c_2}{2}\left(\frac{b_1}{b_2}\frac{\pi}{2}\right)^{-2/3}\left(4\frac{a_1}{a_2} - \frac{b_1}{b_2} - 3\frac{c_1}{c_2}\right)^{5/3}$ and the pattern is stable if and only if $\rho < \min\left(\rho_{K,\text{large}}, \rho_{K,\text{small}}\right)$. The key qualitative difference is that the instability is triggered by small eigenvalues only if $K = 2$; for $K \geq 3$, the large eigenvalues become unstable first. Analytically, the study of large eigenvalues for (8.1) reduces to the following nonlocal eigenvalue problem:

$$\lambda\Phi = \Phi_{yy} + (-1+2w)\,\Phi - \chi w^2 \frac{\int w\phi}{\int w^2}, \quad \chi := \frac{4\sinh^2\left(\frac{L}{\sqrt{D}}\right)}{2\sinh^2\left(\frac{L}{\sqrt{D}}\right) + 1 - \cos\left[\pi(1-1/K)\right]}. \tag{8.5}$$

Its stability has been rigorously and fully characterized in any dimension in [23]; in particular it was shown that the large eigenvalues are stable if and only if $\chi > 1$.

On the other hand, the reduced problem (4.1) is not as well understood: in part, numerical computations were necessary to compute the instability thresholds, and it remains an open problem to justify this fully without relying on numerics. Moreover, unlike for the GM model, the instability of large eigenvalues for (1.2) is due to a Hopf bifurcation (see section 4).

As mentioned in the introduction, in section 5 we computed the instability thresholds $\rho_{K,\text{small}}$ for small eigenvalues indirectly by calculating the bifurcation point at which asymmetric spike patterns bifurcate off the solution branch corresponding to spikes of equal height. These thresholds were then verified numerically; the small eigenvalues themselves were never actually computed. This remains an open problem, although we expect that techniques similar to those used in [4], [19] may work to derive the small eigenvalues and the corresponding instability thresholds in a more systematic manner.

When constructing a spike in two dimensions, we assumed the radial symmetry of the domain. Actually, our main result in two dimensions (Proposition 6.1) still holds even for nonradial domains; the problem then is to determine the location of the spike. For this, a higher order solvability is needed and is left for future work. The various stability thresholds for the two-dimensional problem is also left for future work. Finally, the spike insertion observed in Experiment 4 of section 7 is another interesting and unexplored phenomenon.

Acknowledgments. TK would like to thank the Department of Mathematics at CUHK for their kind hospitality. We thank Professor M. J. Ward and the anonymous referees for their detailed corrections and many constructive suggestions.

REFERENCES

[1] U. Ascher, R. Christiansen, and R. Russell, *A collocation solver for mixed order systems of boundary value problems*, Math. Comp., 33 (1979), pp. 659–579.
[2] S. M. Durant, *Predator avoidance, breeding experience and reproductive success in endangered cheetahs, Acinonyx jubatus*, Animal Behaviour, 60 (2000), pp. 121–130.
[3] S. M. Durant, *Living with the enemy: Avoidance of hyenas and lions by cheetah in the Serengheti*, Behavioral Ecology, 11 (2000), pp. 624–632.
[4] D. Iron, M. J. Ward, and J. Wei, *The stability of spike solutions to the one-dimensional Gierer-Meinhardt model*, Phys. D, 150 (2001), pp. 25–62.
[5] *FlexPDE software*, http://www.pdesolutions.com.
[6] T. Hillen and K. J. Painter, *A user's guide to PDE models for chemotaxis*, J. Math. Biol., 58 (2009), pp. 183–217.
[7] Y. Kan-On, *Stability of singularly perturbed solutions to nonlinear diffusion systems arising in population dynamics*, Hiroshima Math. J., 23 (1993), pp. 509–536.
[8] K. Kishimoto, *Instability of non-constant equilibrium solutions for a system of competition-diffusion equations*, J. Math. Biol., 13 (1981), pp. 105–114.
[9] T. Kolokolnikov, M. Ward, and J. Wei, *Self-replication of mesa patterns in reaction-diffusion models*, Phys. D, 236 (2007), pp. 104–122.
[10] G. L. Lamb, *Elements of Soliton Theory*, John Wiley & Sons, Inc., New York, 1980.
[11] Y. Lou, W.-M. Ni, and S. Yotsutani, *On a limiting system in the Lotka-Volterra competition with cross-diffusion*, Discrete Contin. Dyn. Syst., 10 (2004), pp. 435–458.
[12] Y. Lou and W.-M. Ni, *Diffusion, self-diffusion and cross-diffusion*, J. Differential Equations, 131 (1996), pp. 79–131.
[13] Y. Lou and W.-M. Ni, *Diffusion vs. cross-diffusion: An elliptic approach*, J. Differential Equations, 154 (1999), pp. 157–190.
[14] R. McKay and T. Kolokolnikov, *Stability transitions and dynamics of localized patterns near the shadow limit of reaction-diffusion systems*, Discrete Contin. Dyn. Syst. B, to appear.
[15] M. Mimura and K. Kawasaki, *Spatial segregation in competitive interaction-diffusion equations*, J. Math. Biol., 9 (1980), pp. 49–64.

[16] M. Mimura, Y. Nishiura, A. Tesei, and T. Tsujikawa, *Coexistence problem for two competing species models with density-dependent diffusion*, Hiroshima Math. J., 14 (1984), pp. 425–449.
[17] J. D. Murray, *Mathematical Biology*, Springer-Verlag, Berlin, 1989.
[18] Y. Nishiura and D. Ueyama, *A skeleton structure of self-replicating dynamics*, Phys. D, 130 (1999), pp. 73–104.
[19] H. van der Ploeg and A. Doelman, *Stability of spatially periodic pulse patterns in a class of singularly perturbed reaction-diffusion equations*, Indiana Univ. Math. J., 54 (2005), pp. 1219–1301.
[20] N. Shigesada, K. Kawasaki, and E. Teramoto, *Spatial segregation of interacting species*, J. Theoret. Biol., 79 (1979), pp. 83–99.
[21] M. J. Ward and J. Wei, *Hopf bifurcation of spike solutions for the shadow Gierer–Meinhardt model*, European J. Appl. Math., 14 (2003), pp. 677–711.
[22] M. J. Ward and J. Wei, *Asymmetric spike patterns for the one-dimensional Gierer-Meinhardt model: Equilibria and stability*, European J. Appl. Math., 13 (2002), pp. 283–320.
[23] J. Wei, *On single interior spike solutions of the Gierer-Meinhardt system: Uniqueness and spectrum estimate*, European J. Appl. Math., 10 (1999), pp. 353–378.
[24] J. Wei and M. Winter, *Critical threshold and stability of cluster solutions for large reaction-diffusion systems in* R^1, SIAM J. Math. Anal., 33 (2002), pp. 1058–1089.
[25] Y. Wu, *The instability of spiky steady states for a competing species model with cross diffusion*, J. Differential Equations, 213 (2005), pp. 289–340.
[26] Y. Wu and Q. Xu, *The existence and structure of large spiky steady states for S-K-T competition systems with cross-diffusion*, Discrete Contin. Dyn. Syst., 29 (2011), pp. 367–385.